

CUDA-PIM: End-to-End Integration of Digital Processing-in-Memory from High-Level C++ to Microarchitectural Design

Orian Leitersdorf
Technion – Israel Institute of
Technology
Haifa, Israel
orianl@campus.technion.ac.il

Ronny Ronen
Technion – Israel Institute of
Technology
Haifa, Israel
ronny.ronen@technion.ac.il

Shahar Kvatinisky
Technion – Israel Institute of
Technology
Haifa, Israel
shahar@ee.technion.ac.il

ABSTRACT

Digital processing-in-memory (PIM) architectures mitigate the memory wall problem by facilitating parallel bitwise operations directly within memory. Recent works have demonstrated their algorithmic potential for accelerating data-intensive applications; however, there remains a significant gap in the programming model and microarchitectural design. This is further exacerbated by the emerging model of partitions, which significantly complicates control and periphery. Therefore, inspired by NVIDIA CUDA, this paper provides an end-to-end architectural integration of digital memristive PIM from an abstract high-level C++ programming interface for vector operations to the low-level microarchitecture.

We begin by proposing an efficient microarchitecture and instruction set architecture (ISA) that bridge the gap between the low-level control periphery and an abstraction of PIM parallelism into warps and threads. We subsequently propose a PIM compilation library that converts high-level C++ to ISA instructions, and a PIM driver that translates ISA instructions into PIM micro-operations. This drastically simplifies the development of PIM applications and enables PIM integration within larger existing C++ CPU/GPU programs for heterogeneous computing with significant ease.

Lastly, we present an efficient GPU-accelerated simulator for the proposed PIM microarchitecture. Although slower than a theoretical PIM chip, this simulator provides an accessible platform for developers to start executing and debugging PIM algorithms. To validate our approach, we implement state-of-the-art matrix operations and FFT PIM-based algorithms as case studies. These examples demonstrate drastically simplified development without compromising performance, showing the potential and significance of CUDA-PIM.

1 INTRODUCTION

As the memory wall [21, 38] continues to limit the performance of data-intensive applications, processing-in-memory (PIM) solutions are rapidly emerging to enable logic functionality within the computer memory. The read/write memory interface is supplemented with logic operations where the CPU requests that the memory perform vectored logic on data residing at given addresses, thereby dwarfing data transfer. Whereas early proposals for PIM [12, 37] integrated computation elements *near* memory arrays, emerging PIM proposals exploit the same physical devices for both storage and logic.

Emerging digital PIM architectures enable bitwise operations within the memory with massive parallelism by designing logic

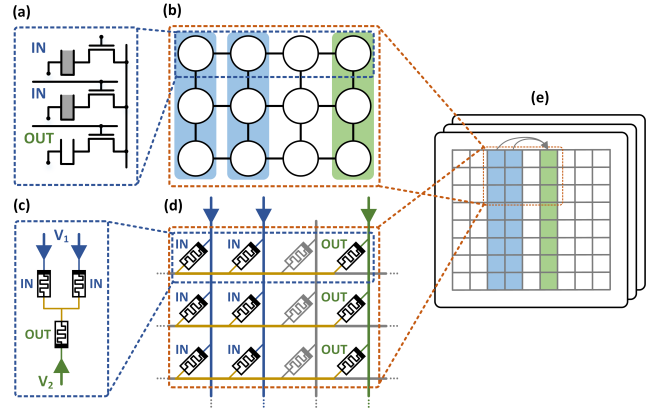


Figure 1: (a) Majority logic [13, 18, 33, 43] integrated within (b) all rows of a DRAM subarray. (c) Stateful logic [7, 15, 26, 41, 48, 50] between memristors within (d) all rows of a memristive crossbar array. Both support (e), an abstract model enabling arbitrary bitwise operations on columns. The figure is adapted from AritPIM [28].

circuits from the same underlying physical devices that construct the memory. For example, DRAM PIM [13, 18, 33, 43] exploits the circuit found in Figure 1(a) to perform majority logic between the capacitors. The circuit from Figure 1(a) is found in every column¹ of the DRAM subarray, thereby enabling parallel execution of the same logic gate amongst all aligned columns in the subarray and all subarrays in the memory. Similarly, memristive [10] memories enable logic functionality according to the circuit in Figure 1(c) [7, 15, 26], which can then similarly be repeated across all rows of a crossbar array for massive throughput [48, 50]. Unlike DRAM PIM, memristive PIM also simultaneously supports parallel operations across columns due to the symmetry of memristor arrays. The parallelism of memristive PIM may be further increased through partitions [2, 15, 28, 31, 35]. Therefore, as a case study, we propose in this paper a framework that supports *partition-enabled memristive PIM* as the most complex case. Future works may adapt this framework to other digital PIM technologies such as non-partitioned memristive PIM [7, 26, 34], DRAM PIM [13, 18, 33, 43], SRAM PIM [1, 11], and FeFET [3, 40].

The algorithmic challenge in utilizing the potential of digital PIM arises from the efficient utilization of the massive bitwise

¹The sub-array is illustrated transposed in Figure 1(b).

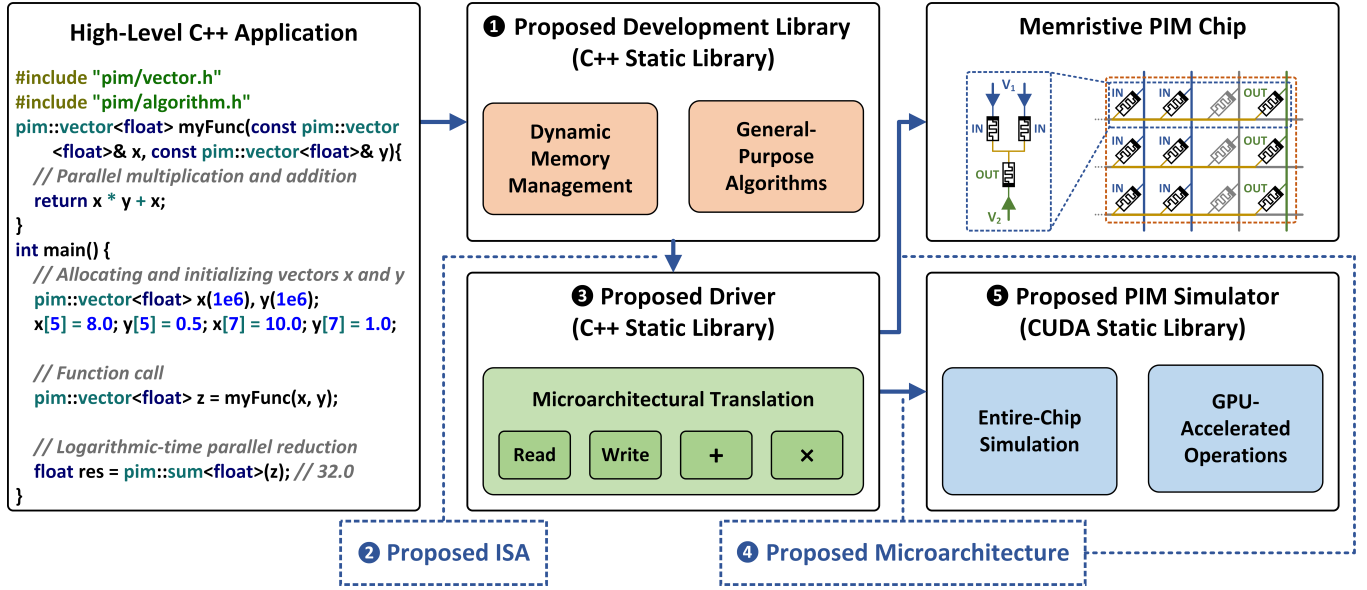


Figure 2: End-to-end integration from high-level C++ programs to the underlying proposed microarchitecture (arrows indicate runtime dependencies), thereby enabling the development and debugging of PIM applications. The high-level C++ code primarily utilizes bindings for `pim::vector` that are converted into ISA instructions by the development library, and then into micro-operations by the PIM driver.

parallelism. Since the gates can only be performed in parallel when they are aligned, we strive to design algorithms that maximize the gate alignment throughout the computation. The first algorithmic step involves constructing high-throughput *vectorized* arithmetic from the underlying basic bitwise operations. AritPIM [28] recently proposed a suite of high-throughput arithmetic operations for both fixed-point and floating-point numbers that is based on the *element-parallel* approach for performing vectored arithmetic in parallel across all rows of the memory. The next step expresses applications such as matrix multiplication [30] and Fast-Fourier-Transforms (FFT) [27] in terms of these vectored arithmetic operations, while also manually managing the vector alignment in the memory.

While significant effort has been invested in the algorithmic development of digital PIM, there have been only a few works on the underlying microarchitecture, controller design, and programming model. This paper aims to provide the end-to-end architectural integration for memristive PIM that intends to bridge the gap between high-level algorithmic theory and low-level logic design. Figure 2 is an overview of this goal, providing a familiar C++ development environment for the algorithmic theory that is automatically translated into the parallel low-level operations which adhere to the proposed microarchitecture. This is accomplished by first designing an efficient microarchitecture and instruction-set-architecture (ISA) that support the massive PIM parallelism, and then proposing a combination of both a PIM library that provides the high-level C++ bindings while also, e.g., managing PIM memory allocations, and a PIM driver responsible for micro-operation generation. We further propose a GPU-accelerated digital PIM simulator that models the proposed microarchitecture as a drop-in replacement for the physical chip. This enables a ready-to-use platform for high-level

development and debugging of PIM algorithms. Overall, CUDA-PIM is the culmination of the following five contributions:

- **Development Library 1:** We propose a PIM development library that enables high-level C++ applications (seen on the left of Figure 2) to automatically exploit PIM parallelism. The library includes dynamic memory management and C++ operator overloading techniques that enable PIM development with ease and are seamlessly integrated within existing C++ programs for heterogeneous computing. Furthermore, our library enables the design of new PIM routines (e.g., `myFunc` in Figure 2) using traditional C++ semantics, and we provide general-purpose routines such as vector reduction (summation) in logarithmic time [42] using `pim::sum`.
- **Instruction Set Architecture (ISA) 2:** Inspired by CUDA, we propose a theoretical model for digital PIM that enables arithmetic register operations on warps and threads (corresponding to crossbars and rows, respectively) and aims to express the digital PIM parallelism in a fashion that abstracts the implementation details (e.g., the supported logic gates) while maintaining the massive throughput. This both simplifies algorithmic development and enables the same instructions to be applied to different PIM architectures.
- **Host Driver 3:** We propose an efficient driver that translates macro-instructions into micro-operations, supporting the AritPIM [28] algorithms on both fixed-point and floating-point numbers. While previous works assumed that this translation is performed via a dedicated hardware controller, we design an efficient host program that supports the massive PIM parallelism. This provides far greater

flexibility than a hardware controller, as the driver may be easily modified in the future for additional functionality.

- **Microarchitecture ④:** We propose a comprehensive microarchitecture for digital memristive PIM that addresses efficient operation decoding for partitions, flexible crossbar addressing, and flexible row isolation. This is accomplished first through a variety of novel techniques that express the wide range of possible partition operations with a minimal number of bits, and then through a standardization of the operation format between the host driver and the PIM chip.
- **GPU-Accelerated Simulator ⑤:** We develop an optimized digital PIM simulator that interfaces with the host driver as a replacement for the physical digital PIM chip. The simulator is itself developed in CUDA to reduce simulation time and enable the simulation of large-scale applications. Overall, the simulator enables the execution, debugging, and profiling of large-scale PIM applications with ease.

This paper is organized as follows. We begin in Section 2 with general background on memristive digital PIM and a summary of the related architectural works. We then continue in Section 3 by proposing a comprehensive PIM microarchitecture that supports partitions, and in Section 4 we propose an abstract PIM ISA inspired by the CUDA model of threads and warps. In Section 5, we propose the development and the driver libraries that enable digital PIM algorithm development with significant ease, and in Section 6 we evaluate the libraries using the proposed GPU-accelerated simulator and demonstrate example applications with no latency overhead and identical correctness. Section 7 discusses miscellaneous considerations, and Section 8 concludes this paper.

2 BACKGROUND

This section begins by providing background on digital memristive PIM architectures from both the circuit and the theoretical algorithmic perspectives, and then continues with a review of the previous architectural concepts.

2.1 Digital Memristive PIM

Digital memristive PIM architectures [9, 15, 22, 32, 42, 47, 48, 50] utilize the emerging nonvolatile memristor device [10, 44] towards a dense computer memory that is inherently capable of both information storage and digital logic. Stateful logic [41], the underlying logic technique for memristors, provides the foundation for high-throughput bitwise operations that are then extended towards parallel vectored arithmetic operations [6, 16, 28, 31, 35]. These high-throughput vectored operations may be utilized towards tackling applications such as matrix operations [30], neural network inference and training [22, 23], genome sequencing [14, 24], graph operations [32], and Fast Fourier Transforms (FFT) [27].

The memristor is a nonvolatile two-terminal resistive device that is inherently capable of both information storage and digital logic. Memristors possess a variable resistance that is modified through a strong current – typically, a current in one direction may increase the resistance, whereas a current in the opposite direction decreases it. Therefore, memristors support binary information storage through their resistance where the resistance

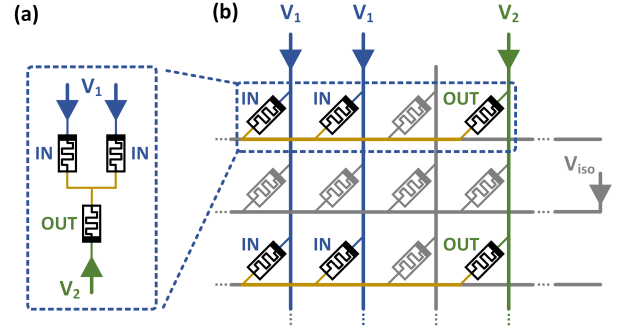


Figure 3: (a) Stateful logic [41] in the resistance domain between three memristors. (b) Parallel stateful logic in a crossbar array by applying V_1 and V_2 across bitlines while skipping a row using V_{iso} .

domain is split into a binary classification (high resistance for logical zero and low resistance for logical one). Writing is performed with a relatively high current, whereas reading is performed by measuring the current from a low voltage. Furthermore, stateful logic [7, 15, 26, 41] enables logic operations between memristors in the resistance domain by applying fixed voltages. Consider the circuit in Figure 3(a) assuming $V_1 \gg 0V$, $V_2 = 0V$, and that the output memristor is initialized to low resistance: only if the resistance of at least one of the input memristors is low (logical one), then a strong current will flow through the output memristor and switch it to high resistance (logical zero). That is, a logical NOR is performed between the resistance states of the input memristors, with the result stored in the output memristor [26]. This logic technique has been extensively studied from the circuit perspective and already has several experimental demonstrations across different memristive devices [7, 19, 20, 45, 51].

Memristive crossbar arrays enable high-density memories that also support parallel stateful logic operations. Such crossbar arrays are typically formed from a grid of, e.g., 1024×1024 memristors connected to vertical bitlines and horizontal wordlines, as seen in Figure 3(b). Write operations are performed by grounding a specific wordline and then applying a high voltage across the bitline(s) of the corresponding memristor(s). Read operations are performed similarly, albeit with a lower applied voltage and with a current sense amplifier connected to the bitline(s). Lastly, logic operations are performed by applying the fixed voltages V_1 and V_2 on three arbitrary bitlines, leading to the circuit seen in Figure 3(a) forming in all rows of the crossbar *in parallel*. By broadcasting the same instruction to (up to) all of the crossbars in the overall memory, this parallelism may be extended to massive throughput for aligned bitwise operations. It is also possible to *skip* (deselect) rows in stateful logic by, for example, applying an isolation voltage V_{iso} to the corresponding wordline.

The element-parallel arithmetic technique extends the bitwise parallelism towards high-throughput vectored arithmetic. Consider a crossbar of dimensions $h \times w$ containing two h -dimensional N -bit vectors \vec{u}, \vec{v} , where each row contains a single element from each vector. This technique performs a vectored operation (e.g., vector addition) on \vec{u}, \vec{v} in parallel across all rows. The *bit-serial*

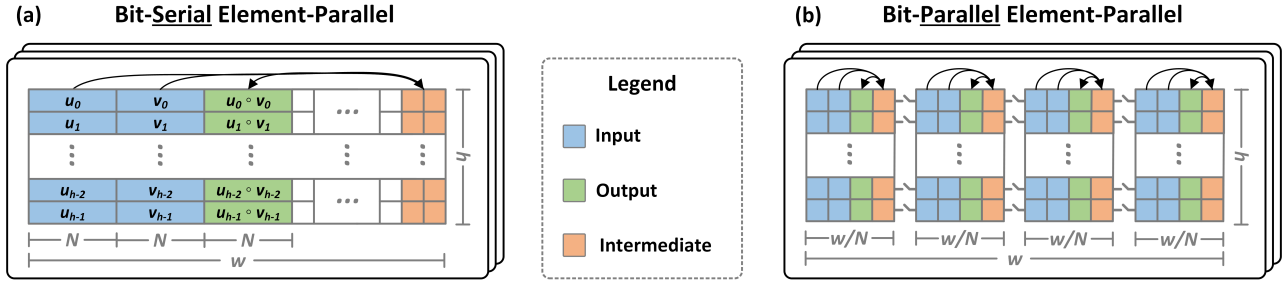


Figure 4: (a) Bit-serial element-parallel arithmetic constructs vectored arithmetic from a serial sequence of logic gates that is performed in parallel across all rows (one gate per row in every cycle). Conversely, (b) the bit-parallel element-parallel approach stores the vectors in a *strided* format across N partitions (each bit position in a different partition) and performs N gates per row per cycle.

element-parallel approach [6, 16, 28, 48], illustrated in Figure 4(a), accomplishes this task by expressing the arithmetic operation as a serial sequence of logic gates and then executing the sequence in parallel across all rows. For example, N -bit addition is performed by first constructing a one-bit full-adder from 9 serial NOR gates, and then implementing ripple-carry addition in $9N$ cycles. While this approach possesses long latency, it also provides high throughput from the concurrent execution across all rows. Conversely, the *bit-parallel* element-parallel [28, 31, 35] approach strives to provide both low latency and higher throughput by introducing dynamically-connected (transistor-based) *partitions* that enable multiple gates per row per cycle. For example, with N partitions, the vectors can be stored in a bit-strided format, as shown in Figure 4(b). When the partitions are disconnected, the maximal parallelism of N gates per row is possible in every cycle; the partitions may also be connected to allow gates between different partitions, enabling information transfer between them. This may accelerate arithmetic through algorithms such as carry lookahead [28] by enabling up to N concurrent gates for each arithmetic operation, e.g., reducing N -bit multiplication latency from $O(N^2)$ to $O(N \log(N))$ (14 \times improvement for $N = 32$ [28]). Essentially, this reduces the latency from the total gate count toward the critical path length.

Such high-throughput arithmetic is exploited towards the acceleration of data-intensive applications. These applications can be broadly split into intra-crossbar and inter-crossbar. Intra-crossbar applications focus on extending the vector parallelism within a single crossbar to tackle more complex problems, such as matrix operations [17, 22, 30] and Fast-Fourier-Transform (FFT) [27], where the application is primarily expressed as a sequence of vectored arithmetic operations and the data layout within the crossbar is carefully managed to guarantee data alignment. Conversely, inter-crossbar applications utilize the entire memory towards a larger application, such as neural networks [22, 23], graph operations [32], DNA sequencing [14, 24], and databases [39]. Inter-crossbar applications typically consist of intra-crossbar routines performed in parallel across all crossbars, supplemented with data transfer (i.e., read and write) between crossbars.

Crucially, the development of these applications currently requires significant expertise in the low-level design of the bitwise operations that serves as a barrier for the introduction of future

applications. Therefore, we provide a familiar C++ development environment that abstracts PIM implementation details such as dynamic memory layout and logic design.

2.2 Related Works

Previous architectural research into digital PIM primarily focused on designing and evaluating the peripheral circuitry rather than the programming model. Talati *et al.* [46, 48] thoroughly investigated the circuit and peripheral considerations, including the effect of non-ideal wires on the logical correctness and the design of the peripheral circuits that apply the stateful logic voltages [46, 48]. Further, RACER [50] recently continued this work, evaluating additional electrical considerations and designing peripheral circuits for an entire memristive memory architecture. *Yet, there remains a lack of a “CUDA-like” PIM programming framework that enables high-level application development* [33]. Therefore, in this work, we assume the electrical and peripheral correctness from these previous works and instead focus on the microarchitecture and its extension to the high-level C++ programming interface.

There has also been initial development of the micro-operation format and controller design for digital PIM [18, 39, 49, 50]. Yet, the previous micro-operation formats do not support partition-based computation or flexible crossbar/row isolation. Moreover, while the extension to an ISA for arithmetic was also investigated [18, 50], this did not include the CUDA-inspired abstraction proposed in this paper or additional considerations such as dynamic memory management that are necessary for high-level C++ development. Lastly, while previous works have designed on-chip controllers [18, 39, 50], we propose a host driver that both provides greater flexibility (as the driver may be updated without replacing the hardware) and attains the performance required for memristive PIM.

3 MICROARCHITECTURE

This section details the proposed microarchitecture for digital memristive PIM. The microarchitecture supports efficient operation encoding for partitions, flexible range-based crossbar addressing, and flexible range-based row isolation. The micro-operations in this microarchitecture (referred to as “operations” for simplicity) are generated by the host driver proposed in Section 5 and are broadcasted to all crossbars. As the micro-operations directly translate

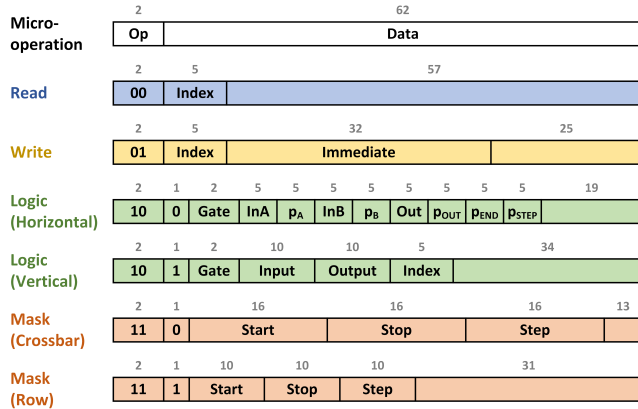


Figure 5: An overview of the different micro-operation types.

into the voltages for the crossbar periphery, then the on-chip controller only needs to buffer the micro-operations from the host driver and broadcast them to the crossbars. We begin with an overview of the microarchitecture and the supported micro-operations in Section 3.1 and Figure 5, and then continue by detailing each type.

3.1 Overview

The proposed microarchitecture supports four different operation types that enable both memory and logic functionality. For simplicity, we present here the case of 1024×1024 crossbars with $N = 32$ partitions comprising an 8GB memory (64k crossbars) [28, 42] that supports NOT and NOR operations in the horizontal direction and NOT operations in the vertical direction. Regardless, the libraries provided in Section 5 can be configured according to different parameters, there are sufficient unused bits in the format for larger memories, and the proposed mechanisms can be generalized to the case where N differs from 32, or the number of partitions differs from N . The interface of the microarchitecture consists of 64-bit operations sent from the host driver, with an optional N -bit response for read operations. The operation types are as follows.

- (1) *Mask*: These operations set the per-crossbar and per-row masks, indicating which rows are active in the following read/write and logic operations.
- (2) *Read/Write*: Standard read/write operations to the memory with N -bit granularity. The target crossbar(s) and row(s) are specified in preceding *mask* operations, and then the intra-row index is specified in the operation.
- (3) *Logic*: These operations communicate a stateful logic operation and are split into *horizontal* operations (as seen in Figure 3) that encode partition operations and *vertical* operations that essentially transfer data between two rows (e.g., using a NOT gate in the transposed direction).

3.2 Mask Operations

These operations select the rows of the memory that will be activated in the following read/write and logic operations. While the maximal PIM throughput is attained when all crossbars and all rows participate in the computation, it may be required to only

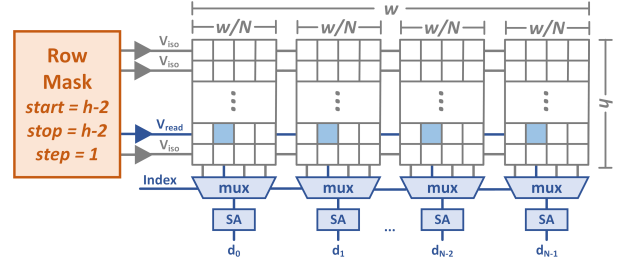


Figure 6: An overview of the reading mechanism [46].

operate on selected crossbars or rows (e.g., using isolation voltages, see Section 2.1) to either avoid corrupting unselected data or reduce energy consumption. We support a range-based pattern for these masks, defined according to *start*, *stop* and *step* values as $\{start, start + step, start + 2 \cdot step, \dots, stop\}$. This pattern enables the flexibility required by previous PIM application works and requires a small representation size.

The crossbar mask is implemented, with every crossbar storing a single volatile bit representing whether that crossbar is currently activated. Whenever a crossbar mask operation is broadcasted, the peripheral circuitry of every crossbar updates the stored activation bit accordingly. For the following non-mask operations, the stored activation bit acts as an enable bit for the entire operation (i.e., the operation is not performed in the given crossbar if the stored activation bit is false).

The row mask is implemented by the crossbars storing the *start*, *stop*, and *step* values and utilizing them in read/write and logic operations. The row mask is updated with a row mask operation that applies to all crossbars and provides the updated *start*, *stop*, and *step* values. During read/write and logic operations, the row mask is expanded into a binary vector of length 1024 representing the activated rows and is then used as the enable bits for the desired operation (for example, whether to apply V_{iso} for stateful logic operations).

3.3 Read/Write Operations

The read/write operations enable standard memory access in addition to the PIM functionality. The operations access the data in N -bit granularity in a strided memory format, where preceding mask operations first selects the desired crossbar(s) and the row(s), and then the read/write operation specifies the intra-row index. Read operations are performed following mask operations that select a single row in a single crossbar and further provide a $\log(w/N)$ -bit index specifying the intra-row strided address. Figure 6 exemplifies this case for $N = 4$ where row $h - 1$ is selected at index 2. The strided memory access is due to the sense amplifiers being shared amongst several consecutive bitlines to reduce area [46, 50], yet this also coincides with the strided memory format utilized in bit-parallel element-parallel computation as there is a single multiplexer for each partition. Write operations are performed similar to Figure 6, yet the mask may select multiple crossbars and rows to enable parallel write operations for the same data.

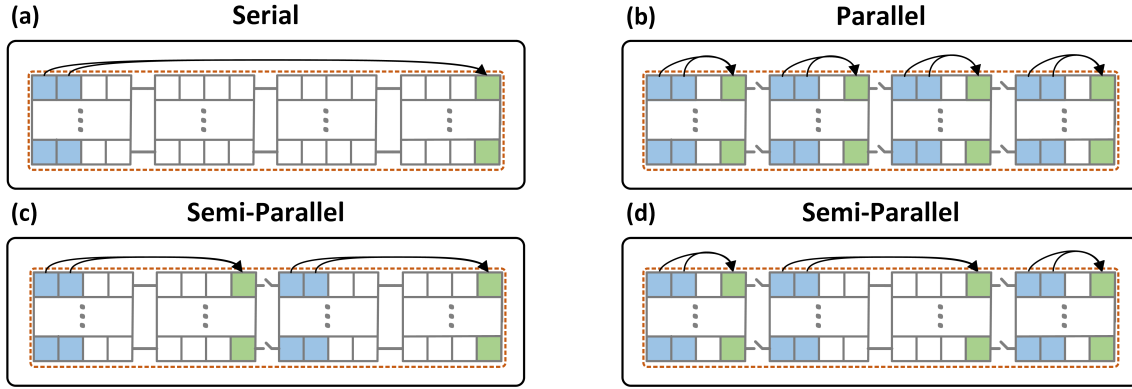


Figure 7: Overview of the different types of partition-based parallelism: (a) serial, (b) parallel, and (c,d) semi-parallel. The dynamic section division is shown in dashed orange, inputs are blue, and outputs are green.

3.4 Logic Operations (Horizontal)

We propose an operation format for encoding partition operations. We begin in Section 3.4.1 with a review of the different forms of partition parallelism (serial, semi-parallel, and parallel) from the perspective of the theoretical computational model [2, 28, 31, 35], continue in Section 3.4.2 by proposing an operation format that supports the full flexibility of partitions (*flexible*), and then conclude in Section 3.4.3 with a special case of the flexible operation format that maintains the support of the previous arithmetic algorithms while providing a significantly smaller operation size (*minimal*).

3.4.1 Partition Parallelism. Partitions enable a unique parallelism that may be exploited for efficient arithmetic techniques. Consider inserting $N - 1$ transistors at fixed locations into each row of an $h \times w$ crossbar, as illustrated in Figure 7. The transistors dynamically isolate different parts of each row to enable concurrent execution, essentially dynamically dividing the crossbar partitions into *sections* (dashed orange) such that each section may perform a parallel stateful logic operation. Initial works [2, 15, 35] utilized partitions in a binary fashion: either the entire crossbar is one section (serial – see Figure 7(a)) or each partition is a section (parallel – see Figure 7(b)). Recent works [28, 31] demonstrated the potential of semi-parallelism, significantly improving binary solutions, e.g., over $4\times$ improvement for multiplication [28, 31, 35]. We define these parallelism forms, presenting a trade-off between parallelism (gates per cycle per row) and flexibility (inputs and outputs from different partitions to facilitate communication between bit positions):

- **Serial** (Figure 7(a)): When the transistors are *all conducting*, the crossbar is equivalent to one without partitions. Thus, only a single gate is executed per row per cycle.
- **Parallel** (Figure 7(b)): When the transistors are *all not conducting*, then N gates may operate concurrently as part of an operation, *one gate within each partition*, or N gates per row per cycle.
- **Semi-Parallel** (Figures 7(c,d)): When only *some* transistors are *conducting*, then multiple gates may operate concurrently, *between partitions*. Essentially, the sections that define the concurrent gates must not intersect (this definition requires fine-tuned controls proposed in this work).

3.4.2 Flexible Partition Model. We propose an efficient operation format for the flexible model, which supports the full flexibility of partition parallelism presented in Section 3.4.1. We begin with background on the operation format in a crossbar without partitions, and then introduce the technique of *half-gates* that enables a simple operation format that may be implemented with efficient control and peripheral circuits. While the proposed operation format requires a large number of bits, we demonstrate through a combinatorial analysis that this is nearly optimal for the flexible model. In Section 3.4.3, we propose a special case of the flexible model that utilizes the same technique of *half-gates* yet further reduces the operation length to the 64-bit format.

The traditional operation format for horizontal logic in non-partition crossbars includes three-column indices that specify the input and output bitlines. Further, the operation also specifies the gate type to be performed; similar to previous works [28, 48, 50], without loss of generality, we assume gates $\{INIT0, INIT1, NOT, NOR\}$, where $INITx$ is a constant logic gate without inputs that sets the output to x (similar to a write operation). The periphery for such a crossbar consists of a column decoder that receives the indices InA , InB , and Out , and applies V_1 on bitlines InA/InB and V_2 on bitline Out , as illustrated in Figure 8(a); the voltages V_1 and V_2 are chosen according to the gate. The column decoder consists of three decoders, each of which receives a single index and output either V_1 or V_2 [5, 41, 46].

Our proposed approach is based on a novel technique of *half-gates*: we utilize a single-column decoder per partition, and introduce per-partition opcodes that are exploited towards partition parallelism, as shown in Figure 8(b). We describe the basic idea through the following example: to support a stateful logic gate where inputs are in partition p_a and outputs are in partition p_b (both in the same section), (1) the column decoder of p_a applies only the input voltages without applying the output voltages, and (2) the column decoder of p_b applies only the output voltages without applying the input voltages. Essentially, p_a “trusts” that a different partition will apply output voltages, and p_b “trusts” that a different partition will apply input voltages. While each gate on its own is not valid (*half-gate*), their combination is valid. Table 1 details

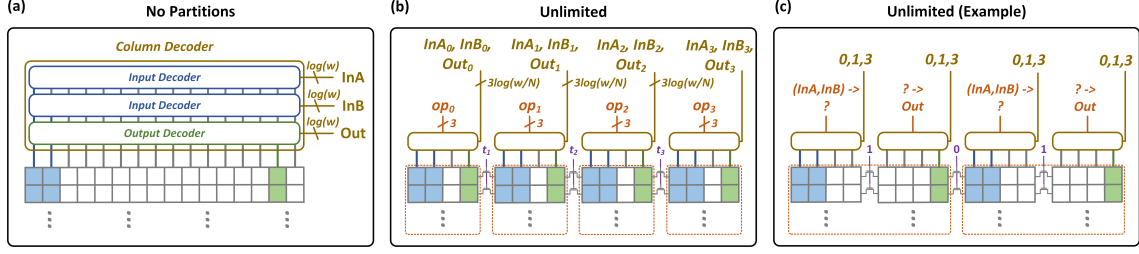


Figure 8: (a) The stateful logic periphery for a baseline crossbar with no partitions [46]. (b) The proposed approach based on the half-gates technique, with (c) an example for semi-parallelism corresponding to Figure 7(c).

Index	Opcode	Index	Opcode
000	-	100	$(InA, ?) \rightarrow ?$
001	$? \rightarrow Out$	101	$(InA, ?) \rightarrow Out$
010	$(?, InB) \rightarrow ?$	110	$(InA, InB) \rightarrow ?$
011	$(?, InB) \rightarrow Out$	111	$(InA, InB) \rightarrow Out$

Table 1: Per-partition opcodes in the half-gate technique.

the various possible opcodes for each column decoder, where “?” represents not applying voltages for that part of the gate and “-” represents not applying voltages at all (e.g., for partitions in between p_a and p_b). An example is shown in Figure 8(c) for the operation from Figure 7(c). The opcode decoding utilizes the first two bits as the enable bits for the input decoders, and the last bit as the enable bit for the output decoder.

This operation format requires $2 + 3N \cdot \log(w/N) + 3N + (N - 1) = 609$ bits in total (gate type, intra-partition indices, partition opcodes, and transistor selects), a $19\times$ increase over the operation length for a crossbar without partitions. There are over 2^{443} different operations possible in the flexible model,² and thus we find that the long operation format is primarily due to the inherent high flexibility of the model.

3.4.3 Minimal Partition Model. This section proposes three restrictions on the flexible model that greatly reduce the operation length while having no impact on the performance of the previous algorithmic PIM works as they already adhere to these patterns.

The first restriction requires identical *intra-partition* indices; that is, $InA_0 = InA_1 = \dots$, $InB_0 = InB_1 = \dots$, $Out_0 = Out_1 = \dots$. The example in Figure 8(c) already satisfies this requirement as the same $InA, InB, Out = 0, 1, 3$ are inputted to all of the column decoders. Notice that, as in the case of Figure 8(c), some of the inputs are not utilized by the partitions (e.g., a partition with opcode $(InA, InB) \rightarrow ?$ will not use Out), yet this does not affect the operation correctness.

The second restriction is that the opcodes repeat periodically. Consider the opcodes representing the leftmost gate (e.g., the opcodes of $(InA, InB) \rightarrow ?$ and $? \rightarrow Out$ in the first and second partitions of Figure 8(c), respectively). We require that the opcodes for the remaining concurrent gates in the operation repeat; e.g., the

opcodes in the third and fourth partitions in Figure 8 are a repetition of the opcodes in the first and second partitions. The operation encoding includes (1) the partition indices p_A, p_B, p_{OUT} of the two inputs and the output of the leftmost gate (where $p_A \leq p_B$), and (2) the periodicity represented by the index of the partition containing the output of the last gate p_{END} and the repetition step size p_{STEP} .

The third restriction aims to deduce the transistor selects from the opcodes. The partition model as defined above enabled some flexibility in the selection of the transistor selects for the same set of gates. For example, if there are two concurrent gates, one from partition 0 to partition 3 and another from partition 8 to partition 11, then any one of the transistors between partition 3 and partition 8 can be set to non-conducting for the operation to be valid. For the case of $p_A \leq p_{OUT}$ ($p_A > p_{OUT}$ is similar), we restrict the transistor selects to adhere to the following pattern: a transistor is set to non-conducting only if the partition to its left has opcode $* \rightarrow Out$ (where $*$ reflects “don’t care”) or the partition to its right has opcode $(InA, *) \rightarrow *$. This restriction enables the generation of the transistor selects from the other existing fields.

Overall, we find that the minimal operation format requires $2 + 3 \cdot \log(w) + 2 \cdot \log(N) = 42$ bits in total (gate type, input/output indices, and opcode pattern), only a $1.31\times$ increase over the operation length for a crossbar without partitions. We present the overall operation format in Figure 5, providing 19 unused bits in the 64-bit operation format.

We find that this *minimal* operation model still supports the full flexibility of the previous algorithmic works as it supports the underlying fundamental routines utilized in those works. Previous works that have utilized the high flexibility of semi-parallelism have first designed useful general-purpose partition techniques such as broadcast and reduction operations [28, 31], and have then utilized those routines to tackle larger problems such as parallel prefix carry-lookahead addition [28]. As the operations utilized in the general-purpose partition techniques adhere to the minimal partition model, we find that this model may also support the more complex arithmetic algorithms. We demonstrate this in Sections 5 and 6 by implementing the AritPIM [28] suite using the proposed microarchitecture which adheres to the minimal model.

3.5 Logic Operations (Vertical)

Stateful logic also supports operations in the transpose direction when the voltages V_1, V_2 are applied on the wordlines rather than the bitlines [48]. These operations are primarily utilized to transfer

²As $\left[\binom{w/N}{2} \cdot (w/N - 2) \right]^N \geq 2^{443}$ for $w = 1024$ and $N = 32$.

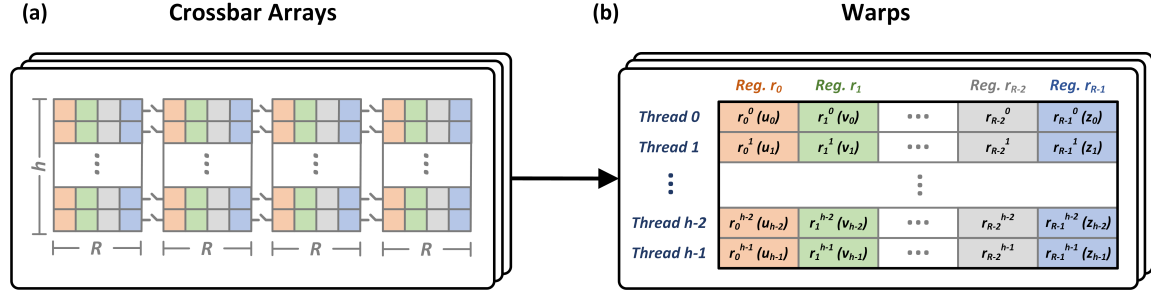


Figure 9: The proposed ISA expresses (a) crossbar arrays as (b) *warps of threads* that may operate concurrently, where each register index may represent an h -dimensional vector (e.g., register r_{R-1} represents the vector \vec{z}).

data between different rows, such as using two consecutive NOT gates [42], as arithmetic in the transpose direction is not possible when N -bit numbers are stored across N horizontal cells. Therefore, we support only the $\{INIT0, INIT1, NOT\}$ set of gates for vertical stateful logic operations. The operation format includes the input and output rows for the vertical gate, as well as the *Index* field that represents the column mask. That is, the vertical logic operation is applied to the columns that are at intra-partition index *Index*, similar to the access pattern of read/write operations.

4 INSTRUCTION-SET ARCHITECTURE

We propose a CUDA-inspired general-purpose PIM instruction set architecture (ISA) that abstracts the implementation details of PIM. The proposed model is based on an abstraction of crossbar arrays as *warps of threads*, where each thread is a single row that contains R N -bit registers.³ Warps are capable of performing R-type (register) macro-instructions (referred to as “instructions” for simplicity) in parallel across (up to) all threads, or serial inter-thread move instructions. This ISA is exploited in the proposed PIM library to enable both (1) an interface for powerful general-purpose vectored operations with significant ease, and (2) the potential for more complex intrinsics utilized in specific circumstances. Similar to CUDA, the proposed library may be utilized without knowledge of the underlying ISA, yet this knowledge is necessary to implement more complex routines efficiently.

The CUDA architecture provides an environment similar to traditional multi-threaded programming by enabling the concurrent execution of the same function by different threads (with potentially different parameters). However, different from traditional CPU multi-threaded programs, the threads are grouped into *warps*. Each warp consists of threads that ideally operate in unison, broadcasting the same instruction to all the threads, where each thread is executed by a separate register file and arithmetic logic unit (ALU) pair. Furthermore, intra-warp data transfer and synchronization are significantly more efficient than instructions between warps, and thus applications aim to maximize locality between threads in the same warp. While it is possible for different threads in the same warp to perform different instructions (warp divergence), this reduces performance as the different instructions are performed

serially. Overall, we find that CUDA programming involves (1) invoking parallel vectored routines through the CUDA interface, (2) specifying the instructions performed by the threads in each warp.

We observe a striking similarity between the CUDA warp model and the parallelism supported by crossbar arrays. Similar to CUDA warps, the threads within a crossbar array may operate concurrently only if they perform the same instruction. Furthermore, intra-crossbar communication is significantly more efficient than inter-crossbar communication as it can be performed in parallel across all crossbars, and thus many applications aim to maximize intra-crossbar instructions. Therefore, we propose in Figure 9 the CUDA-inspired ISA for general-purpose digital PIM computing. We adopt the strided data format from Figure 9(a) to consider each row as a group of R N -bit general-purpose registers in Figure 9(b). Each row represents a single computation thread that operates on the general-purpose registers of that row, and all of the threads in a crossbar array represent a single warp. The proposed ISA differs from CUDA in that the computation is performed *within* the memory; that is, *the registers of the threads are also the memory itself*. For example, consider a simple vectored arithmetic instruction performed on vectors stored in the memory. CUDA would *allocate* threads (in dedicated CUDA cores) that copy the data from the memory to registers, perform the arithmetic on the registers, and then write the results back to the memory. Conversely, the proposed ISA would *activate* the existing threads representing the memory where the vectors are already stored, and those threads would operate directly on the vectors through their registers.

Figure 10 illustrates the two instruction types of the proposed ISA: register (R-type) and move. Register-type instructions represent arithmetic operations on the registers in parallel across (up to) all threads simultaneously, where the activated threads follow the same flexible range-based pattern defined in Section 3 to reduce peripheral complexity. We support the AritPIM [28] suite of arithmetic functions that includes all elementary instructions (addition, subtraction, multiplication, and division) on both fixed-point and floating-point numbers. We further extend the ISA to include comparison operations, bitwise operations, and miscellaneous routines (e.g., absolute value, multiplexing); the full list of supported operations is available in the code repository. Further, the ISA also supports warp-parallel thread-serial move instructions that enable communication between different threads in the same warp. These instructions move a register value from one thread to a different

³We require that the PIM architecture satisfy $w \geq R \cdot N$, and that the ISA and microarchitecture share the same representation width (N).

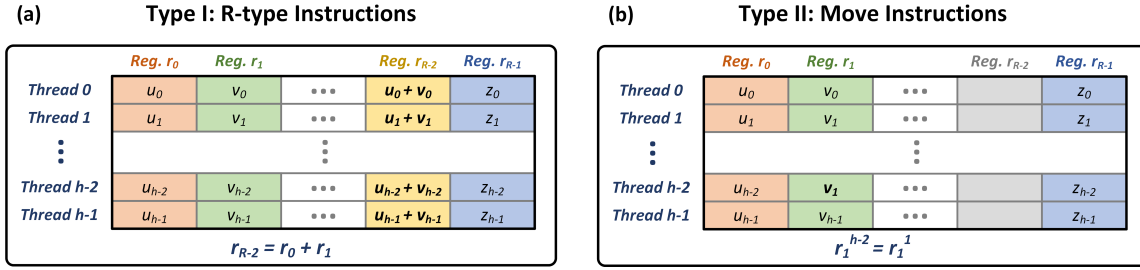


Figure 10: The proposed ISA enables (a) R-type instructions (thread-parallel register operations) and (b) move instructions (serial inter-thread data transfer) within warps of threads, in parallel across (up to) all warps. Note: r_i refers to the register at index i , and u_i, v_i, z_i refer to values.

thread in the same warp, where the registers are aligned. Lastly, the ISA supports standard read and write instructions to the memory. Read instructions are targeted at a single register in a single thread of a single warp, while write instructions also target a single register yet may be repeated across several threads or warps following a range-based pattern.

Overall, the ISA is accessed through the development library of Section 5. ISA knowledge is not required for developing applications such as the program seen in Figure 2, yet such knowledge may assist in optimizing performance.

5 PIM LIBRARY AND HOST DRIVER

We propose development and driver libraries that enable PIM programming with significant ease based on the proposed ISA and microarchitecture. The development library is a C++ static library that provides familiar C++ bindings to the proposed ISA and is responsible for dynamic memory management, whereas the driver efficiently translates the macro-instructions from the development library into micro-operations.

5.1 Development Library

The proposed development library enables the seamless integration of PIM into traditional C++ programs. This both provides a familiar C++ programming interface for PIM, and also enables PIM to be easily integrated within larger applications (e.g., hybrid CPU-PIM or CPU-GPU-PIM development). The development library consists of three different aspects:

- *C++ Bindings*: The development library includes C++ bindings that enable the development of *parallel* digital PIM applications similar to that of traditional serial C++ programs. The example program from Figure 2 demonstrates initialization of PIM vectors (e.g., `pim::vector<float> x(1e6)`), direct read/write access (e.g., `x[5] = 8.0`), the passing of PIM vectors as arguments (e.g., `myFunc`), and parallel arithmetic (e.g., `x * y`).
- *Dynamic Memory Management*: One of the largest challenges with digital PIM is the need for the memory to be properly aligned to enable parallelism; for example, the vectors x and y must be stored in the same warp for $x * y$ to be computed. The development library addresses this

challenge through the combination of (1) a fall-back routine that copies vectors if they are not in the same warp (to avoid throwing an error), and (2) the careful management of PIM vectors that attempts to allocate them consecutively. Specifically, PIM vectors are allocated at a specific register index across the rows of potentially several warps, and the `malloc` routine in the development library aims to map consecutive requests to the same warp ranges. We also provide an explicit routine of `mallocMulti` to enable the user to allocate several aligned vectors in the same warp explicitly.

- *Algorithms*: We include several general-purpose algorithms, including logarithmic reduction [42] and logarithmic prefix [8] that supports both intra-warp and inter-warp cases.

5.2 Host Driver

The host driver is responsible for the translation of the abstract macro-instructions (e.g., register add) into the micro-operations that adhere to the proposed microarchitecture (e.g., logic NOR). While previous works implement this step in a dedicated on-chip controller [18, 39, 50], we propose an efficient host program that is capable of supporting the massive parallelism of digital memristive PIM, as demonstrated in Section 6. The efficiency is due to the combination of efficient low-level implementations of the AritPIM [28] suite of algorithms, and the compact representation for minimal partition operations (Section 3) that maintains minimal data transfer between the host driver and the on-chip controller. The development library and ISA proposed in CUDA-PIM may also be directly applied to different digital PIM architectures by replacing the host driver, *thereby enabling the same high-level PIM application to be applicable to a wide variety of digital PIM architectures*. Moreover, manufacturers of digital PIM architectures may simply adapt the CUDA-PIM host driver according to their specific implementation.

6 EVALUATION

We evaluate CUDA-PIM both from the perspective of the correctness and throughput of the proposed development library and host driver, and from the perspective of the support of the end-to-end architecture for the development of digital PIM applications. We begin by evaluating the proposed libraries: (1) we verify *correctness* through a GPU-accelerated digital PIM simulator that is a drop-in

System	Parameters
Host	CPU: 2x AMD EPYC 7513 (32 core) GPU: NVIDIA A6000 Memory Size: 16x 64GB Memory BW (per chip): 25.6 GB/s
Simulated PIM [28]	Memory Size: 8GB Crossbars: 1024×1024 (32 partitions) Representation Size (N): 32 Clock Frequency: 333 MHz

Table 2: The evaluation parameters for CUDA-PIM.

replacement for a digital PIM chip, and (2) we evaluate *performance* by measuring the maximal throughput supported for the micro-operation generation in the host. Lastly, we demonstrate the *applicability* of CUDA-PIM through the implementation simplicity of two state-of-the-art digital PIM applications. The proposed libraries are available in the code repository⁴. Table 2 lists the parameters used in the evaluation, including both the host system on which the libraries are executed and the parameters for the digital PIM architecture simulated by the proposed simulator that are adopted from previous works [28, 42, 50].

6.1 Correctness

We evaluate the correctness of the proposed end-to-end integration from the high-level C++ code to the generated sequence of micro-operations through a digital PIM simulator. The simulator is a drop-in replacement for a digital PIM chip, thereby verifying that the proposed libraries lead to the intended results when paired with a digital PIM architecture. We follow the previously-established standard of cycle-accurate simulation [16, 27, 28, 30, 36], which requires that (1) the only interaction between the simulator and the library is through the interface for micro-operations, (2) the simulator models the operations cycle-by-cycle and executes them the same as a digital PIM chip, and (3) the results are compared to the intended output as generated by a trusted traditional CPU-only program. Since we are simulating an entire PIM memory (in contrast to previous works that only simulated single rows or crossbars), we also accelerate the simulation time by using a CUDA-enabled GPU and exploiting two optimizations:

- *Memory*: The simulator stores the state of the digital PIM chip in the GPU memory – the logical states of all rows of all crossbars. Whereas previous works stored each row as a vector of Booleans (effectively stored as bytes) [27, 28, 30, 36], our simulator stores rows in a condensed 32-bit format that is defined according to the strided data format.
- *Logic*: We perform the logic operations efficiently by exploiting CUDA bitwise arithmetic operations to perform semi-parallel and parallel operations (rather than iterating over the partitions explicitly). Furthermore, the micro-operations are performed in batches to improve the memory locality of each crossbar in the simulator.

⁴Available at <https://github.com/oleitersdorf/CUDA-PIM>.

We design a set of high-level C++ unit tests that test the different ISA instructions (available in the code repository), and execute them with the proposed simulator. The results are identical to the expected output generated by a CPU-only program, including an exact comparison for IEEE 754 floating-point standards (i.e., IEEE 754 rounding is implemented exactly).

6.2 Throughput

We evaluate the throughput of the proposed development library and host driver compared to the theoretical maximal throughput of digital memristive PIM. The main concern is that the CPU-based translation of macro-instructions into micro-operations may cause a bottleneck since (1) CPUs are not optimized for the bit manipulations required in generating micro-operations, and (2) the operation data transfer between the CPU and the digital PIM chip is larger when the communication is via micro-operations rather than macro-instructions.

We demonstrate the efficiency of the proposed libraries through the maximal operation throughput supported. We utilize the unit tests from Section 6.1 to measure the peak operation throughput that can be produced by the libraries (that is, the maximal throughput at which the micro-operations can be generated by the host driver). This is measured by replacing the digital PIM simulator by the host driver writing the micro-operations to the host memory (to reflect a scenario where the host driver is the bottleneck). This evaluation methodology evaluates both the CPU generation of micro-operations and the operation data-transfer as the micro-operations are written to the host memory. The results are highlighted in Figure 11 in terms of arithmetic throughput for a variety of AritPIM [28] ISA functions, demonstrating that a single-threaded execution of the driver produces operations at a throughput that is 6.4× higher than the maximal throughput at which the digital PIM architecture can consume the operations. Therefore, we find that the host driver is indeed not the bottleneck, and is capable of generating the micro-operations faster than they are required by the digital PIM architecture. We further evaluate the potential performance from 128-threaded execution of the host driver for an extension of CUDA-PIM that supports different warps executing different instructions (supported by utilizing multi-threaded CPU code that calls the same CUDA-PIM development library from different threads). We find that the multi-threaded throughput is 95× higher than digital PIM and is near the bound from the maximal theoretical throughput of the host memory ($16 \times 25.6 \text{ GB/sec} = 409.6 \text{ GB/sec}$). Therefore, CUDA-PIM supports digital PIM parallelism for up to 95 divergent warps with no performance impact.

6.3 Applicability

Lastly, we demonstrate the effectiveness of the proposed abstraction by implementing two state-of-the-art PIM algorithms above the development library. We begin with MatPIM [30], a recent work on the acceleration of matrix-multiplication and two-dimensional convolution via digital memristive processing-in-memory. Whereas the original cycle-accurate simulator of MatPIM was implemented directly in low-level NOR operations, we implement MatPIM above CUDA-PIM – thereby drastically simplifying code design. We then

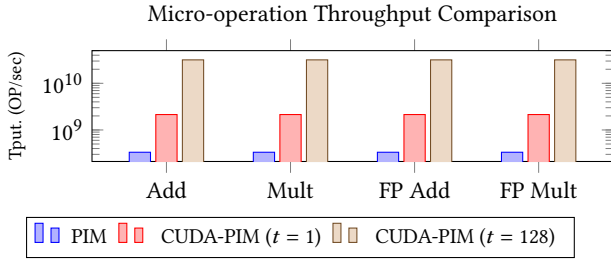


Figure 11: The throughput comparison for CUDA-PIM between the peak throughput produced by the host driver ($t = 1$ for single-threaded and $t = 128$ for multi-threaded) compared to the maximal throughput consumed by digital PIM described in Table 2.

continue with FourierPIM [27], which accelerates the Fast-Fourier-Transform (FFT), and similarly demonstrates drastically simpler code that retains the same correctness and latency. The implementations of both applications are available in the code repository, with the code reduction highlighted in the README. CUDA-PIM does not introduce an abstraction gap (i.e., does not require additional operations that would be otherwise unnecessary) for these applications as the applications are arithmetic-based and thus already utilized the AritPIM algorithms; rather, CUDA-PIM provides a drastically simpler programming interface that maintains performance.

7 ADDITIONAL CONSIDERATIONS

We present in this section several miscellaneous considerations and limitations of CUDA-PIM.

- (1) **Virtual Memory:** While CUDA-PIM does not explicitly support memory virtualization, future work may add this capability by either: (1) providing software virtualization through the memory controller library, or (2) utilizing the same hardware mechanisms present in traditional memory virtualization after the controller – where pages correspond to warps (e.g., 128KB pages).
- (2) **Reliability and Endurance:** There is an ongoing effort in addressing the reliability and endurance of memristors for digital PIM. For example, recent works exploited in-memory error-correcting-code (ECC) and triple-modular-redundancy (TMR) towards improved reliability [25, 29]. CUDA-PIM does not exacerbate the problem with either reliability or endurance, and such reliability techniques can also be integrated into the host driver. Regardless, the same concepts proposed in CUDA-PIM may be applied to other architectures such as DRAM PIM [13, 18, 43].
- (3) **Parameter Exposure:** While the proposed ISA abstracts away the low-level details of the digital PIM architectures, the warp size parameters and the number of registers in each thread are directly related to the array size. We address this limitation by adding the `pim::warpSize()` function that returns the warp size of the current architecture and enables the simultaneous optimization of general PIM programs for different digital PIM architectures. Further, CUDA-PIM requires that the internal mechanisms and parameters of the digital PIM architecture (e.g., the supported

logic gates) be exposed to the host driver. If the manufacturer does not intend to reveal this information, then the manufacturer may provide an obfuscated [4] driver and interface with the proposed development library.

8 CONCLUSION

As digital PIM architectures continue to emerge, there has been significant work on the algorithmic potential of the underlying parallel computing model – from high-throughput arithmetic to large-scale applications. This paper provides the first end-to-end architectural integration of digital PIM from the low-level micro-operation format to a familiar high-level C++ programming interface. This is accomplished by first proposing a microarchitecture for partition-enabled digital memristive PIM and an abstract instruction set architecture (ISA) based on CUDA, and then developing libraries that enable parallel vectored PIM operations in C++ programs with significant ease. We further propose a GPU-accelerated digital PIM simulator that interfaces with the driver to verify correctness while also enabling efficient testing and debugging. Overall, CUDA-PIM increases the accessibility of PIM to the wider community through a familiar programming interface with a powerful abstraction.

ACKNOWLEDGMENTS

This work was supported by the European Research Council through the European Union’s Horizon 2020 Research and Innovation Programme under Grants 757259 and 101069336.

REFERENCES

- [1] Shaizeen Aga, Supreet Jeloka, Arun Subramaniyan, Satish Narayanasamy, David Blaauw, and Reetuparna Das. 2017. Compute Caches. In *IEEE International Symposium on High Performance Computer Architecture*. 481–492. <https://doi.org/10.1109/HPCA.2017.21>
- [2] Mohsen Riahi Alam, M. Hassan Najafi, and Nima TaheriNejad. 2022. Sorting in Memristive Memory. *ACM Journal on Emerging Technologies in Computing Systems (JETC)* 18, 4, Article 69 (2022), 21 pages. <https://doi.org/10.1145/3517181>
- [3] Hussam Amrouh, Di Gao, Xiaobo Sharon Hu, Arman Kazemi, Ann Franchesca Laguna, Kai Ni, Michael Niemier, Mohammad Mehdi Sharifi, Simon Thomann, Xunzhao Yin, and Cheng Zhuo. 2021. Ferroelectric FET Technology and Applications: From Devices to Systems. In *IEEE/ACM International Conference On Computer Aided Design (ICCAD)*. 1–8. <https://doi.org/10.1109/ICCAD51958.2021.9643578>
- [4] Sebastian Banescu and Alexander Pretschner. 2018. A Tutorial on Software Obfuscation. *Advances in Computers*, Vol. 108. Elsevier, 283–353.
- [5] Rotem Ben Hur and Shahar Kvatinsky. 2016. Memristive memory processing unit (MPU) controller for in-memory processing. In *IEEE International Conference on the Science of Electrical Engineering (ICSEE)*. <https://doi.org/10.1109/ICSEE.2016.7806045>
- [6] Rotem Ben-Hur, Ronny Ronen, Ameer Haj-Ali, Debjyoti Bhattacharjee, Adi Eliahu, Natan Peled, and Shahar Kvatinsky. 2020. SIMPLER MAGIC: Synthesis and Mapping of In-Memory Logic Executed in a Single Row to Improve Throughput. *IEEE Transactions on Computer-Aided Design of Integrated Circuits and Systems (TCAD)* 39, 10 (2020), 2434–2447. <https://doi.org/10.1109/TCAD.2019.2931188>
- [7] Julien Borghetti, Gregory S Snider, Philip J Kuekes, J Joshua Yang, Duncan R Stewart, and R Stanley Williams. 2010. ‘Memristive’ switches enable ‘stateful’ logic operations via material implication. *Nature* 464, 7290 (2010), 873–876.
- [8] Richard P. Brent and H. T. Kung. 1982. A Regular Layout for Parallel Adders. *IEEE Trans. Comput.* C-31, 3 (1982), 260–264. <https://doi.org/10.1109/TC.1982.1675982>
- [9] Zamshe Chowdhury, Jonathan D. Harms, S. Karen Khatamifard, Masoud Zabih, Yang Lv, Andrew P. Lyle, Sachin S. Sapatnekar, Ulya R. Karpuzcu, and Jian-Ping Wang. 2018. Efficient In-Memory Processing Using Spintronics. *IEEE Computer Architecture Letters (CAL)* 17, 1 (2018), 42–46. <https://doi.org/10.1109/LCA.2017.2751042>
- [10] Leon Chua. 1971. Memristor – The missing circuit element. *IEEE Transactions on Circuit Theory (TCT)* 18, 5 (1971), 507–519. <https://doi.org/10.1109/TCT.1971.1083337>
- [11] Charles Eckert, Xiaowei Wang, Jingcheng Wang, Arun Subramaniyan, Ravi Iyer, Dennis Sylvester, David Blaauw, and Reetuparna Das. 2018. Neural Cache:

- Bit-Serial In-Cache Acceleration of Deep Neural Networks. In *ACM/IEEE International Symposium on Computer Architecture*. 383–396. <https://doi.org/10.1109/ISCA.2018.00040>
- [12] Duncan G. Elliott, Michael Stumm, W. Martin Snelgrove, Christain Cojocaru, and Robert Mckenzie. 1999. Computational RAM: implementing processors in memory. *IEEE Design & Test of Computers* 16, 1 (1999), 32–41. <https://doi.org/10.1109/54.748803>
- [13] Fei Gao, Georgios Tziantzioulis, and David Wentzlaff. 2019. ComputeDRAM: In-Memory Compute Using Off-the-Shelf DRAMs. In *IEEE/ACM International Symposium on Microarchitecture (MICRO)*.
- [14] Saransh Gupta, Mohsen Imani, Behnam Khaleghi, Venkatesh Kumar, and Tajana Rosing. 2019. RAPID: A ReRAM Processing in-Memory Architecture for DNA Sequence Alignment. In *IEEE/ACM International Symposium on Low Power Electronics and Design (ISLPED)*. <https://doi.org/10.1109/ISLPED.2019.8824830>
- [15] Saransh Gupta, Mohsen Imani, and Tajana Rosing. 2018. FELIX: Fast and Energy-Efficient Logic in Memory. In *IEEE/ACM International Conference on Computer-Aided Design (ICCAD)*. <https://doi.org/10.1145/3240765.3240811>
- [16] Ameer Haj-Ali, Rotem Ben-Hur, Nimrod Wald, and Shahar Kvatinisky. 2018. Efficient Algorithms for In-Memory Fixed Point Multiplication Using MAGIC. In *IEEE International Symposium on Circuits and Systems (ISCAS)*. <https://doi.org/10.1109/ISCAS.2018.8351561>
- [17] Ameer Haj-Ali, Rotem Ben-Hur, Nimrod Wald, Ronny Ronen, and Shahar Kvatinisky. 2018. IMAGING: In-Memory Algorithms for Image processing. *IEEE Transactions on Circuits and Systems I: Regular Papers (TCAS-I)* 65, 12 (2018), 4258–4271. <https://doi.org/10.1109/TCSL.2018.2846699>
- [18] Nastaran Hajinazar, Geraldo F. Oliveira, Sven Gregorio, João Dinis Ferreira, Nika Mansouri Ghiasi, Minesh Patel, Mohammed Alser, Saugata Ghose, Juan Gómez-Luna, and Onur Mutlu. 2021. SIMDRAM: A Framework for Bit-Serial SIMD Processing Using DRAM. In *ACM International Conference on Architectural Support for Programming Languages and Operating Systems (ASPLOS)*.
- [19] Barak Hoffer, Vikas Rana, Stephan Menzel, Rainer Waser, and Shahar Kvatinisky. 2020. Experimental Demonstration of Memristor-Aided Logic (MAGIC) Using Valence Change Memory (VCM). *IEEE Transactions on Electron Devices (TED)* 67, 8 (2020), 3115–3122. <https://doi.org/10.1109/TED.2020.3001247>
- [20] Barak Hoffer, Nicolás Wainstein, Christopher M. Neumann, Eric Pop, Eilam Yalon, and Shahar Kvatinisky. 2022. Stateful Logic Using Phase Change Memory. *IEEE Journal on Exploratory Solid-State Computational Devices and Circuits* 8, 2 (2022), 77–83. <https://doi.org/10.1109/JXDC.2022.3219731>
- [21] Mark Horowitz. 2014. Computing’s energy problem (and what we can do about it). In *IEEE International Solid-State Circuits Conference Digest of Technical Papers (ISSCC)*. <https://doi.org/10.1109/ISSCC.2014.6757323>
- [22] Mohsen Imani, Saransh Gupta, Yeseong Kim, and Tajana Rosing. 2019. FloatPIM: In-Memory Acceleration of Deep Neural Network Training with High Precision. In *ACM/IEEE International Symposium on Computer Architecture (ISCA)*.
- [23] Hai Jin, Cong Liu, Haikun Luo, Jiahong Xu, Fubing Mao, and Xiaofei Liao. 2022. ReHy: A ReRAM-Based Digital/Analog Hybrid PIM Architecture for Accelerating CNN Training. *IEEE Transactions on Parallel and Distributed Systems (TPDS)* 33, 11 (2022), 2872–2884. <https://doi.org/10.1109/TPDS.2021.3138087>
- [24] Marcel Khalifa, Rotem Ben-Hur, Ronny Ronen, Orian Leitersdorf, Leonid Yavits, and Shahar Kvatinisky. 2021. FilPIM: In-Memory Filter for DNA Sequencing. In *IEEE International Conference on Electronics, Circuits, and Systems (ICECS)*. <https://doi.org/10.1109/ICECS53924.2021.9665570>
- [25] Shahar Kvatinisky. 2021. Making Real Memristive Processing-in-Memory Faster and Reliable. In *International Workshop on Cellular Nanoscale Networks and their Applications (CNNA)*. <https://doi.org/10.1109/CNNA49188.2021.9610786>
- [26] Shahar Kvatinisky, Dmitry Belousov, Slavik Liman, Guy Satat, Nimrod Wald, Eby G. Friedman, Avinoam Kolodny, and Uri C. Weiser. 2014. MAGIC – Memristor-Aided Logic. *IEEE Transactions on Circuits and Systems II: Express Briefs (TCAS-II)* 61, 11 (2014), 895–899. <https://doi.org/10.1109/TCSII.2014.2357292>
- [27] Orian Leitersdorf, Yahav Boneh, Gonen Gazit, Ronny Ronen, and Shahar Kvatinisky. 2023. FourierPIM: High-throughput in-memory Fast Fourier Transform and polynomial multiplication. *Memories – Materials, Devices, Circuits and Systems* 4 (2023), 100034.
- [28] Orian Leitersdorf, Dean Leitersdorf, Jonathan Gal, Mor Dahan, Ronny Ronen, and Shahar Kvatinisky. 2023. AritPIM: High-Throughput In-Memory Arithmetic. *IEEE Transactions on Emerging Topics in Computing (TETC)* (2023), 1–16. <https://doi.org/10.1109/TETC.2023.3268137>
- [29] Orian Leitersdorf, Ben Perach, Ronny Ronen, and Shahar Kvatinisky. 2021. Efficient Error-Correcting-Code Mechanism for High-Throughput Memristive Processing-in-Memory. In *ACM/IEEE Design Automation Conference (DAC)*. <https://doi.org/10.1109/DAC18074.2021.9586324>
- [30] Orian Leitersdorf, Ronny Ronen, and Shahar Kvatinisky. 2022. MatPIM: Accelerating Matrix Operations with Memristive Stateful Logic. In *IEEE International Symposium on Circuits and Systems (ISCAS)*. <https://doi.org/10.1109/ISCAS48785.2022.9937557>
- [31] Orian Leitersdorf, Ronny Ronen, and Shahar Kvatinisky. 2022. MultPIM: Fast Stateful Multiplication for Processing-in-Memory. *IEEE Transactions on Circuits and Systems II: Express Briefs (TCAS-II)* 69, 3 (2022), 1647–1651. <https://doi.org/10.1109/TCSII.2021.3118215>
- [32] Ruihao Li, Shuang Song, Qinzhe Wu, and Lizy K. John. 2020. Accelerating Force-directed Graph Layout with Processing-in-Memory Architecture. In *IEEE International Conference on High Performance Computing, Data, and Analytics (HiPC)*. <https://doi.org/10.1109/HiPC50609.2020.00041>
- [33] Shuangchen Li, Dimin Niu, Krishna T. Malladi, Hongzhong Zheng, Bob Brennan, and Yuan Xie. 2017. DRISA: A DRAM-based Reconfigurable In-Situ Accelerator. In *IEEE/ACM International Symposium on Microarchitecture (MICRO)*.
- [34] Shuangchen Li, Cong Xu, Qiaosha Zou, Jishen Zhao, Yu Lu, and Yuan Xie. 2016. Pinatubo: A processing-in-memory architecture for bulk bitwise operations in emerging non-volatile memories. In *ACM/EDAC/IEEE Design Automation Conference*. 1–6. <https://doi.org/10.1145/2897937.2898064>
- [35] Zhaojun Lu, Md Tanvir Arafin, and Gang Qu. 2021. RIME: A Scalable and Energy-Efficient Processing-In-Memory Architecture for Floating-Point Operations. In *IEEE/ACM Asia and South Pacific Design Automation Conference (ASP-DAC)*.
- [36] Batel Oved, Orian Leitersdorf, Ronny Ronen, and Shahar Kvatinisky. 2022. Hash-PIM: High-Throughput SHA-3 via Memristive Digital Processing-in-Memory. In *IEEE International Conference on Modern Circuits and Systems Technologies (MOCAST)*. <https://doi.org/10.1109/MOCAST54814.2022.9837685>
- [37] David Patterson, Thomas Anderson, Neal Cardwell, Richard Fromm, Kimberly Keeton, Christoforos Kozyrakis, Randi Thomas, and Katherine Yelick. 1997. A case for intelligent RAM. *IEEE Micro* 17, 2 (1997), 34–44. <https://doi.org/10.1109/40.592312>
- [38] Ardan Pedram, Stephen Richardson, Mark Horowitz, Sameh Galal, and Shahar Kvatinisky. 2017. Dark Memory and Accelerator-Rich System Optimization in the Dark Silicon Era. *IEEE Design & Test* 34, 2 (2017), 39–50. <https://doi.org/10.1109/MDAT.2016.2573586>
- [39] Ben Perach, Ronny Ronen, Benny Kimelfeld, and Shahar Kvatinisky. 2022. PIMDB: Understanding Bulk-Bitwise Processing In-Memory Through Database Analytics. *arXiv:2203.10486* (2022).
- [40] Dayane Reis, Michael Niemier, and X. Sharon Hu. 2018. Computing in Memory with FeFETs. In *International Symposium on Low Power Electronics and Design*. Article 24, 6 pages. <https://doi.org/10.1145/3218603.3218640>
- [41] John Reuben, Rotem Ben-Hur, Nimrod Wald, Nishil Talati, Ameer Haj Ali, Pierre-Emmanuel Gaillardon, and Shahar Kvatinisky. 2017. Memristive logic: A framework for evaluation and comparison. In *International Symposium on Power and Timing Modeling, Optimization and Simulation (PATMOS)*. <https://doi.org/10.1109/PATMOS.2017.8106959>
- [42] Ronny Ronen, Adi Eliahu, Orian Leitersdorf, Natan Peled, Kunal Korgaonkar, Anupam Chattopadhyay, Ben Perach, and Shahar Kvatinisky. 2022. The Bitlet Model: A Parameterized Analytical Model to Compare PIM and CPU Systems. *ACM Journal on Emerging Technologies in Computing Systems (JETC)* 18, 2 (2022).
- [43] Vivek Seshadri, Donghyuk Lee, Thomas Mullins, Hasan Hassan, Amirali Boroumand, Jeremie Kim, Michael A. Kozuch, Onur Mutlu, Phillip B. Gibbons, and Todd C. Mowry. 2017. Ambit: In-Memory Accelerator for Bulk Bitwise Operations Using Commodity DRAM Technology. In *IEEE/ACM International Symposium on Microarchitecture (MICRO)*.
- [44] Dmitri B Strukov, Gregory S Snider, Duncan R Stewart, and R Stanley Williams. 2008. The missing memristor found. *Nature* 453, 7191 (2008), 80–83.
- [45] Zhong Sun, Elia Ambrosi, Alessandro Bricalli, and Daniele Ielmini. 2018. Logic Computing with Stateful Neural Networks of Resistive Switches. *Advanced Materials* (2018). <https://doi.org/10.1002/adma.201802554>
- [46] Nishil Talati. 2018. *Design of a Memory Controller to Support PIM Operations Using RRAM*. Master’s thesis. Viterbi Faculty of Electrical Engineering, Technion – Israel Institute of Technology, Haifa, Israel.
- [47] Nishil Talati, Rotem Ben-Hur, Nimrod Wald, Ameer Haj-Ali, John Reuben, and Shahar Kvatinisky. 2020. mMPU – a real processing-in-memory architecture to combat the von Neumann bottleneck. *Applications of Emerging Memory Technology: Beyond Storage* (2020), 191–213.
- [48] Nishil Talati, Saransh Gupta, Pravin Mane, and Shahar Kvatinisky. 2016. Logic Design Within Memristive Memories Using Memristor-Aided loGIC (MAGIC). *IEEE Transactions on Nanotechnology (TNANO)* 15, 4 (2016), 635–650. <https://doi.org/10.1109/TNANO.2016.2570248>
- [49] Nishil Talati, Heonjae Ha, Ben Perach, Ronny Ronen, and Shahar Kvatinisky. 2019. CONCEPT: A Column-Oriented Memory Controller for Efficient Memory and PIM Operations in RRAM. *IEEE Micro* 39, 1 (2019), 33–43. <https://doi.org/10.1109/MM.2018.2890033>
- [50] Minh S. Q. Truong, Eric Chen, Deanyone Su, Liting Shen, Alexander Glass, L. Richard Carley, James A. Bain, and Saugata Ghose. 2021. RACER: Bit-Pipelined Processing Using Resistive Memory. In *IEEE/ACM International Symposium on Microarchitecture (MICRO)*.
- [51] Nuo Xu, Taegyun Park, Kyung Jean Yoon, and Cheol Seong Hwang. 2021. In-Memory Stateful Logic Computing Using Memristors: Gate, Calculation, and Application. *Physica Status Solidi (RRL) – Rapid Research Letters* 15, 9 (2021), 2100208. <https://doi.org/10.1002/pssr.202100208>